Journal of Alloys and Compounds 584 (2014) 369–373

Contents lists available at ScienceDirect

Journal of Alloys and Compounds

journal homepage: www.elsevier.com/locate/jalcom

Investigations on structure, ferroelectric, piezoelectric and energy storage properties of barium calcium titanate (BCT) ceramics

Venkata Sreenivas Puli [a,*], Dhiren K. Pradhan [b], Brian C. Riggs [a], Douglas B. Chrisey [a], Ram S. Katiyar [b]

[a] Department of Physics and Engineering Physics, Tulane University, New Orleans, LA 70118, USA
[b] Department of Physics and Institute for Functional Nanomaterials, University of Puerto Rico, San Juan, PR 00936, USA

ARTICLE INFO

Article history:
Received 13 August 2013
Received in revised form 14 September 2013
Accepted 16 September 2013
Available online 24 September 2013

Keywords:
BCT
Aging
Ferroelectrics
Energy density
Solid state sintering

ABSTRACT

We investigated structural, aging induced ferroelectric, piezoelectric and energy density properties of ceramic $(Ba_{0.70}Ca_{0.30})TiO_3$ (BCT) capacitors that were prepared by the solid-state reaction method. According to X-ray (XRD) data, along with $BaTiO_3$ tetragonal peaks, $CaTiO_3$ rich orthorhombic peaks were also observed at room temperature. Raman scattering gives evidence for the formation of oxygen vacancies in BCT due to partial migration of Ca^{2+} into Ti^{4+} site. Abnormal double like hysteresis polarization-electric field (P–E) loops were observed at room temperature for naturally aged BCT ceramics. Strain-electric field (S–E) loops confirm piezoelectric behavior. Room temperature (300 K) charge curve and discharge curve energy densities [$(Ed)_c \sim 0.35$ (before aging) 0.39 J/cm^3 (aged)], [$(Ed)_d \sim 0.20$ (before aging) 0.24 J/cm^3 (aged)], respectively, at a maximum electric field ~50 kV/cm. The bulk BCT materials have shown interesting energy densities with good energy storage efficiency (~58% before aging, ~61% after aging) suggesting they might be strong candidates for high energy density capacitor applications.

1. Introduction

Barium titanate ($BaTiO_3$ or BT)-based materials have been extensively studied for their interesting electrical properties like high dielectric constant, low dielectric loss, ferroelectric, piezoelectric and pyroelectric behavior. Among the dielectric ferroelectric perovskite oxides, BT was used most for electrical and electronic applications, in the years immediately after its discovery. Perovskite oxides derived from BT have a wide range of applications in electronic appliances, such as positive temperature coefficient devices, pulse generating devices, infrared detectors, voltage tunable devices in microwave electronics, multilayer ceramic capacitors, actuators, and lead-free piezoelectric transducers, and charge storage devices [1,2]. Recently, research attention turned towards lead-free and environmentally-friendly dielectric $BaTiO_3$ based piezoelectric materials because of its high dielectric constant, polarization and high piezoelectric properties [3]. BT based high dielectric constant materials with low dielectric loss and high dielectric breakdown field are useful in energy storage capacitors.

Doping is an effective way to improve the electrical performance of electroceramics [4,5]. For instance, barium zirconium titanate $Ba(Zr,Ti)O_3$ [BZT], and barium calcium titanate $(Ba,Ca)TiO_3$ [BCT] [4–6,8] are widely used in electrical material applications. Also, these materials are attracting attention as ceramic capacitors in which the temperature dependence and reliability of the dielectric properties of the BT are improved [6,7]. BCT solid solutions are specifically used in multilayer ceramic capacitor applications and in various other applications like: dielectric filters, antennas, resonators, duplexers and phase shifters, and piezoelectric actuators [8]. Ca^{2+} can occupy either Ba^{2+} site or Ti^{4+} site in $BaTiO_3$ lattice. Ca^{2+} substitution in the Ti^{4+} site requires charge compensation by creating oxygen vacancies in $Ba(Ca_xTi_{1-x})O_{3-x}$ [7]. However the site occupancy mechanism in $BaTiO_3$ is still not completely understood. Ca is known to have solubility upper limit of $x \sim 25$ mol.% on A site doping and an upper limit of $x \sim 4$ mol.% on B-site doping in $BaTiO_3$ [9,10]. Oxygen vacancies are created by charge compensation mechanism and this might be the reason for Ca^{2+} (ionic radius $r_{Ca} = 0.99$ Å) occupancy at B-site (Ti^{4+} site, ionic radius of $r_{Ti} = 0.60$ Å) in perovskite $BaTiO_3$. The solubility limit of Ca^{2+} occupying B-site ($x \sim 0.04$) in $Ba(Ca_xTi_{1-x})O_3$ [11], is much lower when compared to that of A-site doping, due to the larger ionic radius of Ca^{2+} to that of Ti^{4+} [7].

Aging induced double P–E hysteresis behavior has been previously observed for lead-free perovskite $BaTiO_3$/$(Ba,Sr)TiO_3$ [12], $BiFeO_3$ [13], $KNbO_3$ [14], and $(Na,Bi)TiO_3$-based ceramics [15]. However, not much was reported on BCT ceramics aging behavior and only a few reports were available on Ca^{2+} occupying Ti^{4+} in $BaTiO_3$ lattice with aging behavior [16–19]. Many studies are available on BCT based materials for capacitor applications; but none were found on energy density measurements to our knowledge. Many studies are available on BCT based materials for capacitor

* Corresponding author. Tel.: +1 239 537 4964; fax: +1 504 862 8702.
E-mail addresses: vpuli@tulane.edu, pvsri123@gmail.com (V.S. Puli).

0925-8388/$ - see front matter © 2013 Elsevier B.V. All rights reserved.
http://dx.doi.org/10.1016/j.jallcom.2013.09.108

applications; but none were found on energy density measurements to our knowledge. Here in, we report structure, Raman spectra, ferroelectric, piezoelectric and energy density measurement of BCT ceramics for capacitor applications.

2. Experimental procedure

High-purity $BaCO_3$ (99%), $CaCO_3$ (99%), TiO_2 (98%) (Alfa Aesar, U.S.A) powders were used as the starting materials. $(Ba_{0.70}Ca_{0.30})TiO_3$ ceramics were prepared by the conventional solid state reaction of $BaCO_3$, $CaCO_3$ and TiO_2. Stoichiometric quantities of starting materials were ball-milled in a polyethylene jar for 4 h using ZrO_2 balls with ethanol. The mixtures were heated at 800 °C in air for 3 h after drying and sieving. The mixture was calcined at 1250 °C for 10 h. The calcined powder was ball milled and dried again to obtain homogeneous powder. The granulated powders were pressed into disks of 13 mm in diameter and 0.5 mm in thickness using 5% PVA binder, binder burnt out by heating at 500 °C for 1 h and then sintered at 1500 °C in air for 6 h. X-ray diffraction (XRD) patterns at room temperature were obtained on an automated Rigaku D/max 2400 X-ray diffractometer with rotating anode using Cu Kα radiation. After polishing, the dimensions were measured before silver electrodes were deposited on the pellets, then the specimens were fired at 810 °C for 1 h. The Raman measurements were performed using an ISA T64000 triple monochromator. An optical microscope with an 80× objective was used to focus 514.5 nm radiations from a Coherent Innova 99 argon ion laser on the sample. Laser power of ~10 mW was focused on a ~2 μm spot. The same microscope objective collected the backscattered radiation. The scattered light, dispersed by the spectrophotometer, was detected by using a 1 inch charge-coupled device (CCD) detection system with 1800 grooves/mm grating and the spectral resolution was typically <1 cm^{-1}. Ferroelectric hysteresis loops was measured at 50 Hz, with poled disk-shaped samples under an electric field using Radiant Technologies high voltage amplifier (RT 6000 HVA-4000V). Dielectric breakdown voltage of the samples was measured at room temperature using a Trek high voltage amplifier (Trek Inc., Model 30kV/20A).

3. Results and discussion

Fig. 1 shows the room temperature XRD patterns obtained from $(Ba_{0.70}Ca_{0.30})TiO_3$ (BCT) ceramics with angle 2θ (degree) ranging from 10° to 80° with a scan rate of 1° per minute. Tetragonal peaks corresponding to perovskite $BaTiO_3$ and orthorhombic peaks corresponding to $CaTiO_3$ XRD patterns were observed for BCT ceramics with majority of tetragonal phase peaks as reported in previous investigations [20–24] and tetragonal BCT, XRD reflection peaks are isostructural with $Ba_{0.88}Ca_{0.12}TiO_3$ (JCPDS 81-1288). In addition to prominent indexed tetragonal diffraction peaks, orthorhombic peaks corresponding to $CaTiO_3$ were detected at $2\theta = 32.94°$, 47.43°, 58.87°, 69.07° and were indexed with (121), (202), (042) planes respectively. Detected peaks are isostructural with $CaTiO_3$ in complete agreement with JCPDS 75-2100 [24,25]. According to the phase diagram of $BaTiO_3$–$CaTiO_3$ solid solutions prepared by conventional dry route, the formation of $CaTiO_3$ is expected for $x \geqslant 0.16$ at the calcination temperature of 1150 °C [23,26]. In the present study, prolonged calcination (1250 °C/10 h) and sintering (1350 °C/4 h) could not suppress the orthorhombic phase for higher concentrations of calcium in BCT (not shown here). Whereas sintering at higher temperature ~1500 °C/6 h, drastically reduced orthorhombic peaks and whose lattice parameters [($a \sim 3.95191$ Å, $c \sim 3.94950$), tetragonal distortion ($c/a \sim 0.99$) and volume (~61.6817 $Å^3$)] of the unit cell decreased from that of the lower sintering temperature 1350 °C/4 h, [($a \sim 3.958$ Å, $c \sim 4.066$ Å), tetragonal distortion ($c/a \sim 1.027$) and volume (~63.7094 $Å^3$)]. This decrease might be due to partial incorporation of calcium at barium site due to higher sintering temperature (1500 °C) with more dwelling time (6 h). The SEM micrographs of BCT ceramics are shown in Fig. 1 inset. It is found that the sintered ceramics are very dense, uniform void free. The average grain size of the ceramics calculated by line intercept method is around 40–65 μm.

Ferroelectric tetragonal $BaTiO_3$ contain 3A1 + B1 + 4E Raman active phonons; however cubic phase has no Raman active modes in $BaTiO_3$. In brief, room temperature tetragonal $BaTiO_3$ Raman mode were $E(TO_1)$, $A_1(TO_1)$ [sharp mode], $A_1(TO_2)$ [asymmetric broad mode], $B_1/E(TO + LO)$ [sharp mode],$A_1(TO_3)/E(TO_2)$ [asymmetric broad mode], $A_1(LO)/E(LO)$ [asymmetric broad mode]. However much broader and symmetrical [$A_1(TO_2)$, $A_1(TO_3)/E(TO)$, $A_1(LO)/E(LO)$] modes are also present in cubic paraelectric phase, they were often attributed to second-order effects. More precisely, they relate to the disorder of Ti displacements in the TiO_6 octahedra [10]. Raman spectrum in Fig. 2, reveals spectral features at 146 cm^{-1} [$A_1(TO_1)$], 224 cm^{-1} [$A_1(TO_2)$], 297 cm^{-1} [$B_1/E(TO + LO)$], 473 cm^{-1} $A_1(LO_2)/E(LO)$], 524 cm^{-1} [$A_1(TO_3)/E(TO)$], 734 cm^{-1} [$A_1(LO)/E(LO)$], 863 cm^{-1} [A_{1g}]. Similar results were observed in $Ba_{(1-x)}Ca_xTiO_3$, $BaTi_{(1-x)}Ca_xO_3$ ceramic systems [16,27]. The shift of the modes namely [$A_1(TO_3)/E(TO)$, $A_1(LO)/E(LO)$] to higher frequencies when compared to pure and Ca substituted $BaTiO_3$ [27], implies an increase in force constant which resulted from the presence of higher amount of calcium in reaction at the Ba sites. Also the shift of these bands to higher frequencies is attributed to the formation of Ca_{Ba} defects, which is closely related to the phonon vibrations of the Ba–O bonds [27]. Both [$A_1(TO_2)$], [$B_1/E(TO + LO)$] modes at 224 cm^{-1} and 297 cm^{-1} respectively shifted towards lower wave number region, the shift in these two bands to lower wave number region might be caused by the phonon vibrations of Ti–O bonds [27].

These results are in agreement with previous reports on $BaTiO_3$, $Ba_{(1-x)}Ca_xTiO_3$ (BCT), $BaTi_{(1y)}Ca_yO_3$ (BTC) [16,17,27] and simulta-

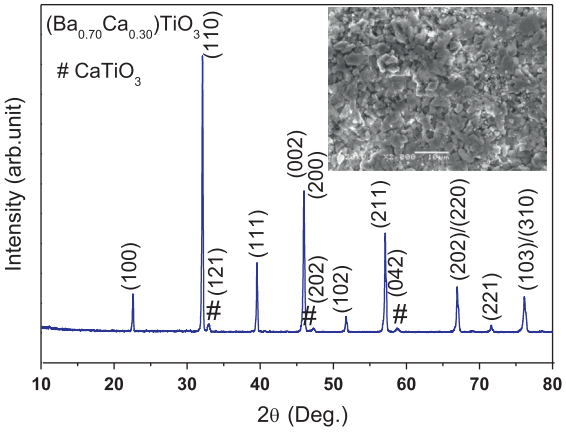

Fig. 1. Room temperature (300 K) slow-scan XRD patterns of $(Ba_{0.70}Ca_{0.30})TiO_3$ (BCT) with 2θ angle ranging 20–80°, scanning electron microscopy image of BCT ceramics (inset).

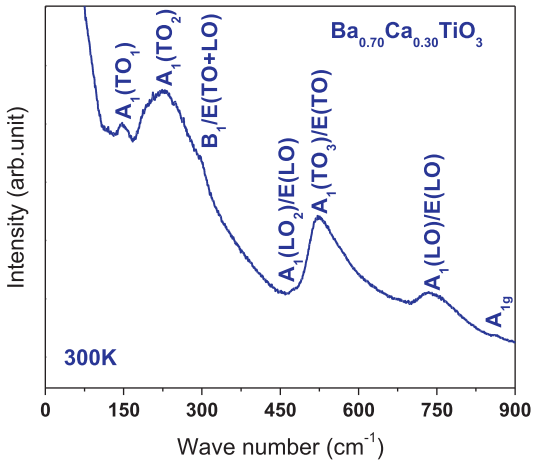

Fig. 2. Room temperature (300 K) unpolarized Raman spectra of $(Ba_{0.7}Ca_{0.3})TiO_3$ – (BCT) ceramics with phonon mode assignments.